

---

# Survival-oriented embeddings for improving accessibility to complex data structures

---

**Tobias Weber**

Department of Statistics  
LMU Munich

tobias.weber@stat.uni-muenchen.de

**Michael Ingrisch**

Department of Radiology  
LMU Munich

michael.ingrisch@med.uni-muenchen.de

**Matthias Fabritius**

Department of Radiology  
LMU Munich

matthias.fabritius@med.uni-muenchen.de

**Bernd Bischl**

Department of Statistics  
LMU Munich

bernd.bischl@stat.uni-muenchen.de

**David Rügamer**

Department of Statistics  
LMU Munich

david.ruegamer@stat.uni-muenchen.de

## Abstract

Deep learning excels in the analysis of unstructured data and recent advancements allow to extend these techniques to survival analysis. In the context of clinical radiology, this enables, e.g., to relate unstructured volumetric images to a risk score or a prognosis of life expectancy and support clinical decision making. Medical applications are, however, associated with high criticality and consequently, neither medical personnel nor patients do usually accept black box models as reason or basis for decisions. Apart from averseness to new technologies, this is due to missing interpretability, transparency and accountability of many machine learning methods. We propose a hazard-regularized variational autoencoder that supports straightforward interpretation of deep neural architectures in the context of survival analysis, a field highly relevant in healthcare. We apply the proposed approach to abdominal CT scans of patients with liver tumors and their corresponding survival times.

## 1 Introduction

Recent developments in survival analysis (SA) have shown a rising interest in the modeling of unstructured data types using deep learning. In medical applications these data types often constitute (volumetric) CT or MRI scans, but other data types such as audio or video signals are also not uncommon. While a majority of deep learning approaches in SA either focus on tabular data [1, 2, 3, 4, 5, 6, 7] or directly apply convolutional neural networks to predict survival based on image data [8, 9, 10], more recent methods such as [11, 12] combine tabular and unstructured information.

**From machine learning research to clinical practice** Given these methodological advancements and the rising interest in artificial intelligence as well as in digital health systems, machine learning models might be used to predict risk scores or patient survival in the near future and play an important role in clinical decision making. This is, however, an application with high criticality and consequently

high requirements for transparency and explainability [13]. Both are considered a must, as model predictions imply decisions such as appropriate therapy measures or a patient’s risk assessment.

Radiology with its comparatively large amounts of unstructured imaging data plays a pivotal role in the digitalization of clinical medicine. As a consequence, numerous efforts have been undertaken to link unstructured imaging data to well defined clinical endpoints such as diagnosis, i.e., image classification, and prognosis, i.e., survival analysis. This is often referred to as radiomics. Since overall survival is an important endpoint in clinical trials, radiomics has also been extended to survival analysis. As in many other domains, deep learning (DL) is a promising candidate for radiological image analysis, but is currently limited in its application. This is not only due to limited sample sizes, but also because of the black-box character of typical DL models. Providing interpretability, explainability and transparency in radiological applications is thus the next important step towards a successful implementation of modern analysis tools in clinical radiology.

**Interpretability methods** Methods for interpretability often analyze and visualize activations in classification or regression tasks to explain the model’s reasoning. For example in [14, 15] gradient-weighted activations are utilized to create a mapping similar to a heatmap that highlights decisive areas in the original image. This is also a useful tool in radiological applications where, e.g., an activation centered in the lung region of a chest X-ray increases trust in a model’s prediction for the presence of pneumonia.

However, to the best of our knowledge, no dedicated tool for the interpretation of models in deep survival learning exists as of now. To close this gap, we propose *CoxVAE* (Fig. 1), a Cox-regularized variational autoencoder (VAE; [16]) that allows for meaningful compression of unstructured data and a straightforward interpretation of the model’s reasoning. Similar to [17], *CoxVAE* utilizes survival label information to produce a survival-optimized embedding that allows to directly assess the importance of the obtained latent features and meaningful processing for subsequent survival downstream applications.

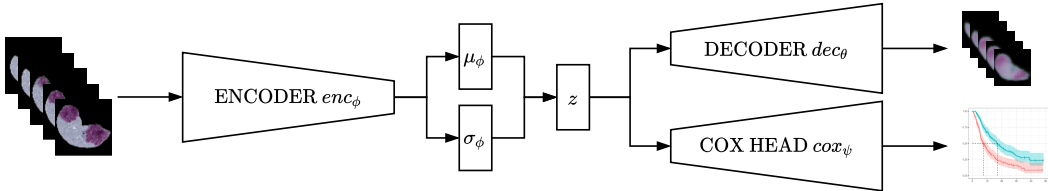


Figure 1: *CoxVAE* multi-task architecture. The encoder  $enc_\phi$  estimates the low-dimensional latent feature distribution  $z|x \sim \mathcal{N}(\mu_\phi, \sigma_\phi^2 \mathbf{I})$  for an arbitrary input  $x$ , e.g., a CT image. Based on the learned embedding  $z$ , the decoder reconstructs the image  $\hat{x}$  while  $cox_\psi$  predicts the patient’s survival by estimating the log-hazard rate based on the corresponding latent sample.

## 2 Survival-oriented embeddings in medical imaging

The VAE is a common and established choice for encoding data. Let  $enc_\phi$  be the probabilistic encoder with parameters  $\phi$  that predicts a latent vector of variables  $z$  with distribution  $z | x \sim \mathcal{N}(\mu_\phi, \sigma_\phi^2 \mathbf{I})$  using a sample  $x \in \mathcal{X}$  from a sample space  $\mathcal{X}$ . Given  $z$ , the decoder  $dec_\theta$  with parameters  $\theta$  creates a reconstruction  $\hat{x}$  of  $x$ . The VAE can be trained by minimizing the negative evidence lower bound (ELBO)

$$\mathcal{L}_{\beta\text{-VAE}}(\theta, \phi; \mathbf{x}) = -\mathbb{E}_{z \sim q_\phi(z|x)} [\log p_\theta(\mathbf{x} | z)] + \beta \mathbb{KL}(q_\phi(z | \mathbf{x}) || p(z)). \tag{1}$$

The ELBO in (1) represents a trade-off between good reconstruction, i.e., maximizing  $\log p_\theta(\mathbf{x}|z)$ , and minimizing the KL-divergence  $\mathbb{KL}$  between the variational density  $q_\phi(z|x)$  and the Gaussian prior  $p(z)$ , controlled by the parameter  $\beta$ . This type of autoencoder is also widely known as  $\beta$ -VAE [18, 19, 20].

**Cox survival objective** The reconstruction of the ( $\beta$ -)VAE induces a latent space that comprises as much information as possible about the data  $x$ , but does not necessarily have an intuitive interpretation. This is, however, a indispensable property when reusing these latent representations in other models

or downstream tasks. Especially for medical applications, an interpretable latent space is crucial and helps clinicians in understanding image features such as detected tumor tissue. To address this need, we propose a CoxVAE framework that extends the base VAE architecture with an additional network head  $cox_\psi$  with parameters  $\psi$ . The network head  $cox_\psi$  itself is a Cox PH model [21] that estimates the log-hazard rate  $r = cox_\psi(\mathbf{z}) \in \mathbb{R}$ . More specifically, for a dataset  $\mathbf{X}$  of  $n$  observations  $(t_i, \delta_i, \mathbf{x}_i)_{i=1, \dots, n}$  with event times  $t_i$ , boolean censoring indicator

$$\delta_i = \begin{cases} 0 & \text{if censored} \\ 1 & \text{else,} \end{cases}$$

and images  $\mathbf{x}_i$ , latent variables  $\mathbf{z}_i \sim q_\phi(\mathbf{z} | \mathbf{x}_i)$  are first generated by the VAE. Based on the negative partial Cox log-likelihood (c.f. [1])

$$\mathcal{L}_{Cox}(\phi, \psi; \mathbf{X}) = -\frac{1}{\sum_{i=1}^n \delta_i} \sum_{i=1}^n \delta_i \left( r_i - \log \sum_{j:t_j \geq t_i} \exp(r_j) \right) \quad (2)$$

and the predicted log-hazard rates  $r_i = cox_\psi(\mathbf{z}_i)$ , the parameters  $\psi$  can be optimized in a second step.

**Combined objectives** Instead of a two-step procedure, we combine the two objectives (1) and (2) and jointly learn the  $enc_\phi$ ,  $dec_\theta$ , and  $cox_\psi$  (schematically depicted in Figure 1). The introduction of a supervised survival loss forces the learned latent space to incorporate the information of the survival labels, which in turn allows for a meaningful compression and better interpretability. As the CoxVAE constitutes a multi-task architecture, we propose to control the balance of both losses via a parameter  $\tau \in [0, 1]$  in the final objective function:

$$\mathcal{L}(\phi, \theta, \psi; \mathbf{X}) = \frac{\tau}{n} \sum_{i=1}^n (\mathcal{L}_{\beta-VAE}(\phi, \theta; \mathbf{x}_i)) + (1 - \tau) \mathcal{L}_{Cox}(\phi, \psi; \mathbf{X}). \quad (3)$$

A large value for  $\tau$  implies a focus on reconstruction, whereas a small value leads to an embedding that strongly influenced by the survival times.

### 3 Survival of cancer patients with liver metastases

We trained the proposed CoxVAE on anonymized contrast-enhanced computed tomography scans of 492 patients with liver metastases. For each patient, the dataset contains an abdominal CT scan and the time until death in days. The overall censoring rate is at 17%.

**Modeling approach** To obtain segmentation masks of the liver, we use the nnU-Net [22]. The CT scan is then downscaled to a resolution of  $64 \times 64 \times 64$  voxels. For  $enc_\phi$  and  $dec_\theta$  we choose neural networks with four residual blocks [23] and a latent space of  $\mathbb{R}^8$ . While the choice of  $cox_\psi$  can be an arbitrary Cox PH model, we found that a linear predictor without bias term yields good results while being inherently interpretable. Another important choice for the model’s performance is the correct balance between the complexity of the two heads  $dec_\theta$  and  $cox_\psi$ . As  $cox_\psi$  in comparison to  $dec_\theta$  only needs a fraction of updates to converge due to the considerably smaller network, we employ two optimizers (Adam; [24]) instead of only one joint optimizer and define different learning rates for both network parts ( $1e-4$  for  $\theta, \phi$  and  $1e-5$  for  $\psi$ ). Training is conducted for 16,000 batch updates with a batch size of 16.

## 4 Results

The main goal of our analysis is to compress CT scans and create an embedding optimized for further survival downstream tasks and straightforward interpretability. While the VAE as unsupervised model has to rely on the visual structures in the supplied images, the CoxVAE is able to incorporate more distinct label information through  $cox_\psi$  in a supervised manner. The results is a completely restructured latent space as depicted in Figure 2. For the vanilla VAE, a PCA dimension reduction of the latent space shows that the main variation in the data does not involve grouping or clusters with

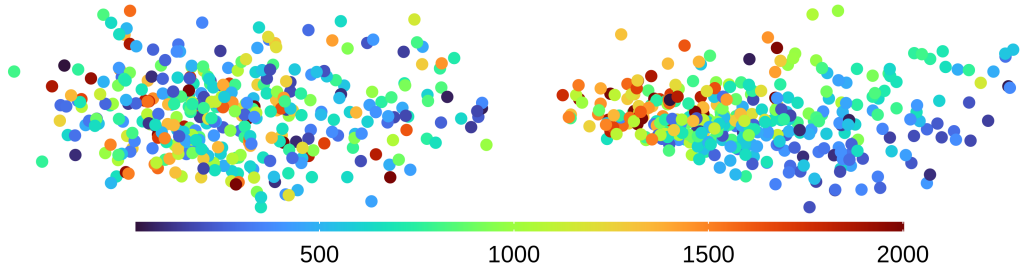


Figure 2: Comparison of the first two PCA components of a VAE (**left**) and a CoxVAE (**right**) embedding for CT imaging data. The color indicates survival time in days. The CoxVAE embedding reflects the learned survival information, whereas the unsupervised VAE shows no apparent grouping.

similar survival times. Instead, data points are mainly clustered based on a visual keys (e.g., the shape and size of the liver). In contrast, the CoxVAE embedding shows a distinct ordering of the PCA’s first component along with decreasing survival times. The focus on visual aspects of the images is a common shortcoming of the VAE, potentially only focusing on low frequency features such as the coarse shape of the liver, whereas high frequency features, e.g., small tumor patches, are often neglected. By employing the additional survival-head, we solve this issue as features that are visually less relevant but crucial for survival receive a greater weight in the total objective (3) (and vice versa).

**Inspecting latent dimensions** While  $cox_{\psi}$  can be chosen to be any Cox PH-based model (e.g., a DeepSurv architecture [1]), using a single linear layer network allows for further insights into the model’s reasoning and its latent space. Being a linear model, a one unit change in the  $i$ -th dimension

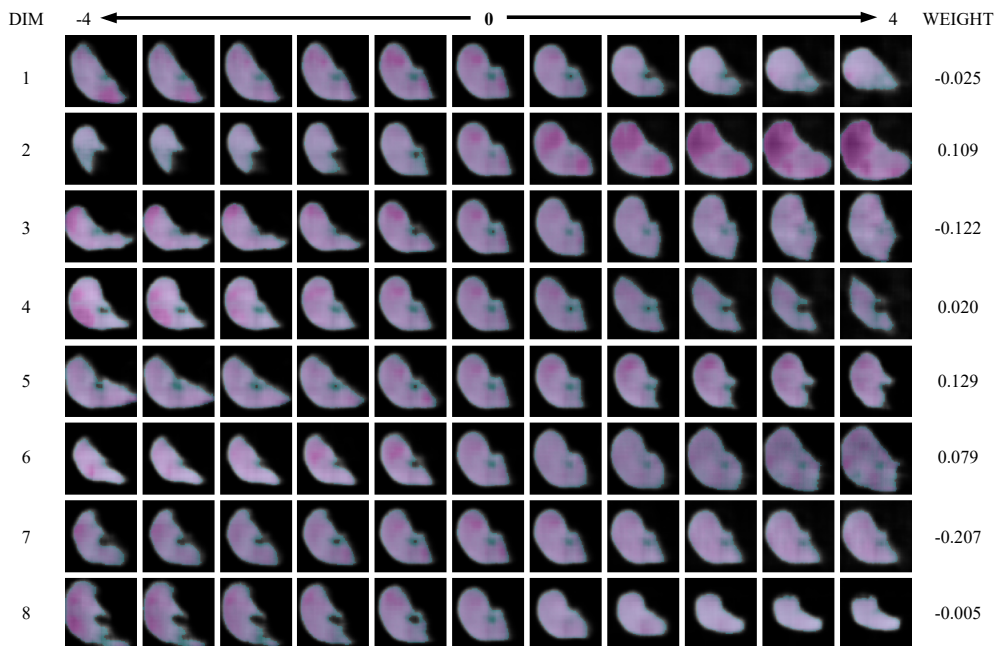


Figure 3: Traversing across all latent 8 latent dimensions in CoxVAE with linear  $cox_{\psi}$ . The images show the reconstruction of different  $z$  of CTs with liver metastases. For reasons of clarity, we only visualize the middle slice of the 3D image. Tumor patches are highlighted with a red overlay. The base  $z$  (**middle column**) is a zero vector. The **columns** model the effect of changing the value in the respective dimensions (**rows**) in the range -4 to 4. On the **right** side the weight of  $cox_{\psi}$  is displayed, that is associated with each dimension. Latent dimensions with a  $cox_{\psi}$  weight close to zero are deemed as rather irrelevant for estimating survival. Large positive weights and large value in  $z$  correspond with a large hazard rate. On the contrary, large negative values result in a high hazard rate when the  $cox_{\psi}$  weight is large negative.

$\psi_i$  of  $\psi$  changes the resulting hazard ratio by a factor of  $\exp(\psi_i)$ . As the latent dimensions are mostly disentangled due to the VAE prior assumption, each dimension can thus be assessed through their importance for the survival outcome and changes in these specific latent features can be represented in  $\mathcal{X}$  by utilizing  $dec_\theta$ . Figure 3 exemplarily depicts this for the CT liver scans with tumor metastases and an 8-dimensional latent space. In this example, dimension 2 of the latent space has an assigned weight of 0.109 (on the log-scale), which translates to an 11.5% increase of the hazard rate per unit change in the latent dimension. As a result, the reconstructed images show a distinct increase and spread of tumor patches along this axis when increasing  $\phi_2$  (or vice versa, decreasing  $\phi_2$  results in disappearing tumor patches).

**Impact of  $\tau$ -parameter** An important parameter in our proposed model is  $\tau$ , which controls the amount of reconstruction as well as the focus on the survival task. Extreme values of  $\tau$  either allow to solely focus on reconstruction or on good survival prediction. In order to investigate its behaviour, we conducted further simulation studies with knowledge of the ground truth based on synthetic MNIST images. Following [25] the synthetic dataset assigns low hazard rates to low digits and vice versa. Figure 4 depicts the evolution of the latent space along different  $\tau$  values. As expected, small values of  $\tau$  imply a strong focus on the survival task, visible by the learned natural order of the digits along the first component of a PCA. An increase of  $\tau$  results in more distinct digit clusters and disentanglement. For large  $\tau$  values, the neighborhood of digits shifts to visual similarities, e.g., the digit 6 is now close to digit 0, whereas 0 and 1 are far away from each other. These results confirm our theoretical presumptions and underline the importance of this parameter. In practice, we recommend choosing  $\tau$  as small as possible (with as much emphasis on the survival task as possible), while ensuring reconstructed images to still look meaningful and interpretable for clinicians.

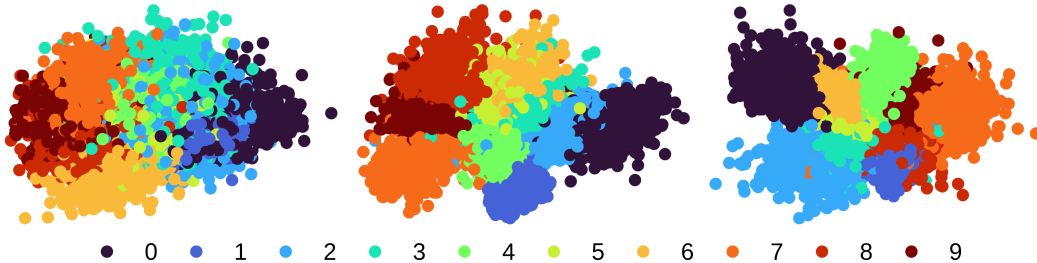


Figure 4: First two PCA-components for encoded surv-MNIST with a  $\tau$  value of 0.01 (**left**), 0.5 (**middle**) and 0.99 (**right**). With increasing  $\tau$  the embedding forms more distinct clusters. The main source of variation changes from the explanation of survival time to structural similarities.

## 5 Practical considerations

An almost omnipresent challenge for the application of survival analysis to radiological imaging data is the limited data size. On the one hand, clinical trials typically only collect tens or hundreds of patients. On the other hand, deep learning-based approaches require a multiple of training data for yielding well-generalizing results with low bias. Although the dataset used in this demonstration is considered large in radiology, fitting a generative deep learning architecture for high-dimensional image data is still challenging. In many applications, it is also not clear, whether unstructured data sources can actually provide predictive information about the survival of patients. Comparisons of our model with DeepSurv [1] and a vanilla VAE embedding imply that our method works similar well with common modeling choices (see Table 1), but also indicate that extraction of information is indeed difficult.

In conclusion, we have demonstrated how a hazard-regularized variational autoencoder can be fitted to unstructured image data, thereby imprinting survival information into the latent space. This latent space is explainable and its relationship with the survival outcome can be easily visualized using the model’s decoder. We demonstrated this approach exemplarily for survival data of cancer patients with metastases in the liver, where the generative model learned that increased risk is associated with increased tumor load.

	C-index ( $\uparrow$ )			IBS ( $\downarrow$ )		
	Base	CoxPH	RSF	Base	CoxPH	RSF
CoxVAE	<b>0.560</b>	0.546	0.558	0.187	0.162	0.169
VAE	–	0.554	0.544	–	0.158	<b>0.153</b>
DeepSurv	0.548	<b>0.560</b>	0.539	0.200	0.162	0.176

Table 1: Validation set results for the CTs with liver metastases using the C-index [26] and integrated Brier score (IBS; [27]). The DeepSurv embedding is obtained by extracting the activations of the last hidden layer. We compute the respective embedding for each model and subsequently fit a Cox PH model and a random survival forest (RSF, [28]) on the obtained latent variables as downstream task. The *base* columns reflect the prediction performance of the architectures themselves.

## References

- [1] Jared L. Katzman, Uri Shaham, Alexander Cloninger, Jonathan Bates, Tingting Jiang, and Yuval Kluger. “DeepSurv: Personalized treatment recommender system using a Cox proportional hazards deep neural network”. In: *BMC Medical Research Methodology* 18.1 (2018).
- [2] Margaux Luck, Tristan Sylvain, Héloïse Cardinal, Andrea Lodi, and Yoshua Bengio. “Deep Learning for Patient-Specific Kidney Graft Survival Analysis”. In: *ArXiv e-prints* (2017). arXiv: 1705.10245.
- [3] Changhee Lee, William R. Zame, Jinsung Yoon, and Mihaela Van Der Schaar. “DeepHit: A deep learning approach to survival analysis with competing risks”. In: *32nd AAAI Conference on Artificial Intelligence, AAAI 2018*. 2018.
- [4] Changhee Lee, William R. Zame, Ahmed Alaa, and Mihaela van der Schaar. “Temporal Quilting for Survival Analysis”. In: *Proceedings of Machine Learning Research*. Ed. by Kamalika Chaudhuri and Masashi Sugiyama. Vol. 89. Proceedings of Machine Learning Research. PMLR, 2019, pp. 596–605.
- [5] Changhee Lee, Jinsung Yoon, and Mihaela Van Der Schaar. “Dynamic-DeepHit: A Deep Learning Approach for Dynamic Survival Analysis with Competing Risks Based on Longitudinal Data”. In: *IEEE Transactions on Biomedical Engineering* 67.1 (2020), pp. 122–133.
- [6] Stefan Groha, Sebastian M. Schmon, and Alexander Gusev. “A General Framework for Survival Analysis and Multi-State Modelling”. In: *ArXiv e-prints* (2020). arXiv: 2006.04893.
- [7] Andreas Bender, David Rügamer, Fabian Scheipl, and Bernd Bischl. “A General Machine Learning Framework for Survival Analysis”. In: *Machine Learning and Knowledge Discovery in Databases*. Springer International Publishing, 2021, pp. 158–173.
- [8] Yucheng Zhang, Edriss M. Lobo-Mueller, Paul Karanicolas, Steven Gallinger, Masoom A. Haider, and Farzad Khalvati. “CNN-based Survival Model for Pancreatic Ductal Adenocarcinoma in Medical Imaging”. In: *ArXiv e-prints* (2019). arXiv: 1906.10729.
- [9] Christoph Haarburger, Philippe Weitz, Oliver Rippel, and Dorit Merhof. “Image-based Survival Analysis for Lung Cancer Patients using CNNs”. In: *Proceedings - International Symposium on Biomedical Imaging 2019-April* (2018), pp. 1197–1201.
- [10] Lin Li, Lixin Qin, Zeguo Xu, Youbing Yin, Xin Wang, Bin Kong, Junjie Bai, Yi Lu, Zhenghan Fang, Qi Song, et al. “Using artificial intelligence to detect COVID-19 and community-acquired pneumonia based on pulmonary CT: evaluation of the diagnostic accuracy”. In: *Radiology* 296.2 (2020), E65–E71.
- [11] Philipp Kopper, Sebastian Pölsterl, Christian Wachinger, Bernd Bischl, Andreas Bender, and David Rügamer. “Semi-structured deep piecewise exponential models”. In: *ArXiv e-prints* (2020). arXiv: 2011.05824.
- [12] David Rügamer, Chris Kolb, and Nadja Klein. “Semi-Structured Deep Distributional Regression: Combining Structured Additive Models and Deep Learning”. In: *ArXiv e-prints* (2021). eprint: 2002.05777.
- [13] Data Ethics Commission, German Federal Ministry of Justice and Consumer Protection. *Opinion of the Data Ethics Commission*. 2019.

- [14] Ramprasaath R. Selvaraju, Abhishek Das, Ramakrishna Vedantam, Michael Cogswell, Devi Parikh, and Dhruv Batra. “Grad-CAM: Why did you say that?” In: *ArXiv e-prints* (2016). arXiv: 1611.07450.
- [15] Aditya Chattopadhyay, Anirban Sarkar, Prantik Howlader, and Vineeth N. Balasubramanian. “Grad-CAM++: Generalized Gradient-based Visual Explanations for Deep Convolutional Networks”. In: *ArXiv e-prints* (2017). arXiv: 1710.11063.
- [16] Diederik P. Kingma and Max Welling. “Auto-encoding variational bayes”. In: *2nd International Conference on Learning Representations, ICLR 2014 - Conference Track Proceedings*. International Conference on Learning Representations, ICLR, 2014.
- [17] Ghalib A. Bello, Timothy J.W. Dawes, Jinming Duan, Carlo Biffi, Antonio de Marvao, Luke S.G.E. Howard, J. Simon R. Gibbs, Martin R. Wilkins, Stuart A. Cook, Daniel Rueckert, and Declan P. O’Regan. “Deep-learning cardiac motion analysis for human survival prediction”. In: *Nature Machine Intelligence* 1.2 (2019), pp. 95–104.
- [18] Alexander A. Alemi, Ian Fischer, Joshua V. Dillon, and Kevin Murphy. “Deep Variational Information Bottleneck”. In: *5th International Conference on Learning Representations, ICLR 2017, Conference Track Proceedings*. 2017.
- [19] Irina Higgins, Loïc Matthey, Arka Pal, Christopher Burgess, Xavier Glorot, Matthew Botvinick, Shakir Mohamed, and Alexander Lerchner. “beta-VAE: Learning Basic Visual Concepts with a Constrained Variational Framework”. In: *5th International Conference on Learning Representations, ICLR 2017, Conference Track Proceedings*. 2017.
- [20] Christopher P. Burgess, Irina Higgins, Arka Pal, Loic Matthey, Nick Watters, Guillaume Desjardins, and Alexander Lerchner. “Understanding disentangling in beta-VAE”. In: *ArXiv e-prints* (2018). arXiv: 1804.03599.
- [21] David R. Cox. “Regression Models with Life Tables”. In: *Journal of the Royal Statistical Society: Series B (Methodological)* (1972).
- [22] Fabian Isensee, Jens Petersen, Andre Klein, David Zimmerer, Paul F. Jaeger, Simon Kohl, Jakob Wasserthal, Gregor Koehler, Tobias Norajitra, Sebastian Wirkert, and Klaus H. Maier-Hein. “nnU-Net: Self-adapting Framework for U-Net-Based Medical Image Segmentation”. In: *ArXiv e-prints* (2018). arXiv: 1809.10486.
- [23] Kaiming He, Xiangyu Zhang, Shaoqing Ren, and Jian Sun. “Deep residual learning for image recognition”. In: *Proceedings of the IEEE Computer Society Conference on Computer Vision and Pattern Recognition*. Vol. 2016-Decem. IEEE Computer Society, 2016, pp. 770–778.
- [24] Diederik P. Kingma and Jimmy Lei Ba. “Adam: A method for stochastic optimization”. In: *3rd International Conference on Learning Representations, ICLR 2015 - Conference Track Proceedings*. International Conference on Learning Representations, ICLR, 2015.
- [25] Michael F. Gensheimer and Balasubramanian Narasimhan. “A scalable discrete-time survival model for neural networks”. In: *PeerJ* 7 (2019), e6257.
- [26] Frank E. Harrell, Robert M. Califf, David B. Pryor, Kerry L. Lee, and Robert A Rosati. “Evaluating the yield of medical tests”. In: *Jama* 247.18 (1982), pp. 2543–2546.
- [27] Erika Graf, Claudia Schmoor, Willi Sauerbrei, and Martin Schumacher. “Assessment and comparison of prognostic classification schemes for survival data”. In: *Statistics in medicine* 18.17-18 (1999), pp. 2529–2545.
- [28] Hemant Ishwaran, Udaya B. Kogalur, Eugene H. Blackstone, and Michael S. Lauer. “Random survival forests”. In: *Annals of Applied Statistics* 2.3 (2008), pp. 841–860.